

# NMR study under pressure on the La1111 pnictides,



N. Fujiwara · T. Nakano · H. Okada · H. Takahashi · Y. Kamihara · M. Hirano · H. Hosono

\*

## Abstract

The relationship between antiferromagnetic (AF) fluctuation and superconductivity was investigated in the La1111 series,  $\text{LaFeAsO}_{1-x}\text{F}_x$  ( $x = 0.05, 0.08, \text{ and } 0.14$ ) by examining nuclear relaxation rates ( $1/T_1$ ) at both ambient pressure and 3.0 GPa. Although the AF fluctuation is enhanced by applying pressure in the underdoped regime ( $x = 0.05, \text{ and } 0.08$ ), the increase in critical transition temperature ( $T_c$ ) is small, whereas  $T_c$  increases remarkably in the overdoped regime ( $x = 0.14$ ) where the AF fluctuation is absent, suggesting that high  $T_c$  above 40 K originates not from the AF fluctuation but from the density of states at the electron pocket.

**KEYWORDS** NMR, High pressure, La 1111 series

PACS numbers:

---

\* N. Fujiwara · T. Nakano

Graduate School of Human and Environmental Studies, Kyoto University, Yoshida-Nihonmatsu-cyo, Sakyo-ku, Kyoto 606-8501, Japan,

e-mail: naoki@fujiwara.h.kyoto-u.ac.jp

H. Okada

Faculty of Engineering, Tohoku Gakuin University, Taga-cho 985-8537, Japan

H. Takahashi

College of Humanities and Sciences, Nihon University, Tokyo 156-8550, Japan

TRiP, Japan Science and technology Agency, Tokyo 102-0075, Japan

Y. Kamihara

Faculty of Science & Technology, Keio University, Yokohama 223-8521, Japan

TRiP, Japan Science and technology Agency, Tokyo 102-0075, Japan

M. Hirano

Frontier Research Center (FRC), Tokyo Institute of Technology, Yokohama 226-8503, Japan

H. Hosono

Materials and Structures Laboratory (MSL), Tokyo Institute of Technology, Yokohama 226-8503, Japan

Frontier Research Center (FRC), Tokyo Institute of Technology, Yokohama 226-8503, Japan

## I. INTRODUCTION

The 1111 series ( $\text{RFeAsO}_{1-x}\text{F}_x$  R=Nd, Sm, Ce, and La, *etc.*) is highly important because its critical transition temperature ( $T_c$ ) is relatively high among iron-based pnictides [1-7]. In the 1111 series, the optimal  $T_c$  is realized away from an antiferromagnetic (AF) phase on the  $T - x$  phase diagram, and the superconductivity is maintained even in a heavily doped regime. These features contrast with those of the 122 series, in which the optimal  $T_c$  appears adjacent to the AF phase [8-10].

In the La1111 series, the optimal  $T_c$  of 26 K appears around  $x = 0.11$ , away from the AF phase. The SC phase is not so sensitive to doping level, but is sensitive to pressure. A clear dome-shaped pressure ( $P$ ) dependence of  $T_c$  has been observed by the resistivity measurements [11, 12]. The highest  $T_c$  is realized by applying pressure to optimally doped ( $x \sim 0.11$ ) or heavily doped ( $x \sim 0.14$ ) samples:  $T_c$  values, 26 and 20 K for  $x = 0.11$  and 0.14, respectively reach to 43 K at a pressure of 4-5 GPa [11, 12]. Structurally, the highest  $T_c$  has been realized when Fe and As ions form regular tetrahedra or the pnictogen height above the basal plane of iron is high [13, 14]. Changes in these parameters resulting from pressure application can modify the band structure and covalency between Fe and As ions, affecting the electronic and/or magnetic properties.

However, the origin of high  $T_c$  in iron-based pnictides is unclear; spin fluctuation seems to be an important factor from an analogy with high- $T_c$  cuprates, while an SC mechanism due to orbital fluctuation has also been suggested [15, 16]. To investigate whether the superconductivity is of magnetic origin as it is in high- $T_c$  cuprates, we measured nuclear magnetic relaxation rates ( $1/T_1$ ) of  $^{75}\text{As}$  systematically under pressure for several doping levels ( $x = 0.05, 0.08$  and  $0.14$ ).

## II. EXPERIMENTAL CONDITIONS

Powder samples were used for the nuclear magnetic resonance (NMR) measurements of  $^{75}\text{As}$ . Field-swept NMR spectra were measured at a fixed frequency of 45.1 MHz. The spectra exhibit a typical powder pattern with two peaks, which is seen under nuclear quadrupole interactions. The relaxation rate  $1/T_1$  was measured at the lower-field peak by the saturation-recovery method. The Fe-As planes contributing to this peak get aligned parallel to the

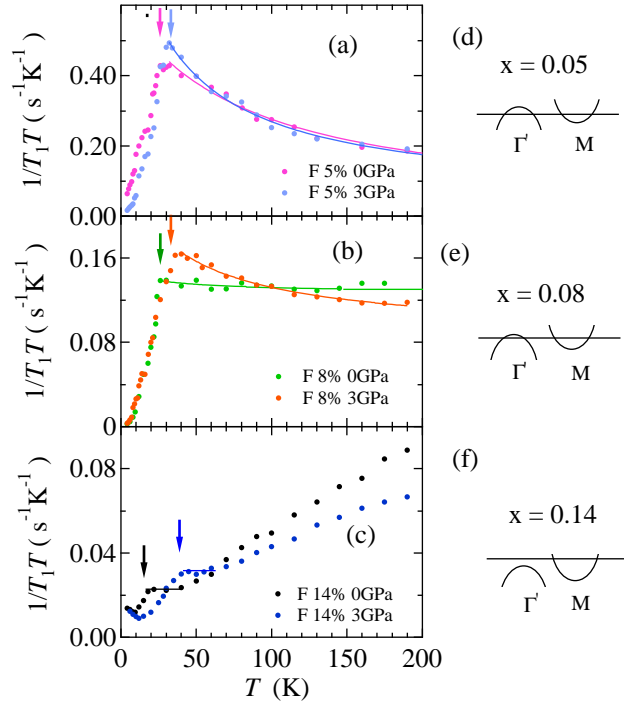


FIG. 1: Relationship between antiferromagnetic (AF) fluctuation and band structure. (a-c) Temperature dependence of  $1/T_1T$  at several doping levels. Arrows indicate  $T_c$  determined from changes in  $1/T_1T$ . (d-f) Schemes of electron and hole pockets. The  $\Gamma'$  point represents  $(\pi, \pi)$  in the unfolded Brillouin Zone. That point overlaps the  $\Gamma$  point corresponding to  $(0, 0)$  in the original folded Brillouin Zone.

applied field.

### III. EXPERIMENTAL RESULTS

Figs. 1(a)-(c) show  $1/T_1T$  measured at ambient pressure and 3.0 GPa for the samples doped with  $x = 0.05$ , 0.08 and 0.14. The data for  $x = 0.08$  and 0.14 were cited from Ref. [17,18]. For the  $x = 0.14$  samples,  $1/T_1T$  has been measured up to 3.7 GPa [18]. At each doping level, qualitatively different features are revealed by applying pressure. Below, we describe in detail what occurs at each doping level.

1) Lightly doped regime ( $x = 0.05$ ). Samples with a very low doping level exhibit clear Curie-Weiss behavior, suggesting that low-frequency AF fluctuation is predominant at this

doping level. The Curie-Weiss behavior is enhanced and  $T_c$  increases slightly at a pressure of 3.0 GPa. The increase  $\Delta T_c$ , indicated by arrows in Fig. 1(a), is estimated as 7-8 K.

2) Underdoped regime ( $x = 0.08$ ). For the  $x = 0.08$  samples, Curie-Weiss behavior is weaker than for  $x = 0.05$  and appears almost independent of  $T$  at ambient pressure. However, Curie-Weiss behavior returns when pressure is applied. The increase in  $T_c$  is almost the same as for  $x = 0.05$ .

3) Over doped regime ( $x = 0.14$ ). For the  $x = 0.14$  samples, the Curie-Weiss behavior completely vanishes at both ambient pressure and 3.0 GPa.  $1/T_1T$  shows a plateau just above  $T_c$  and a monotonous increase with the increase in temperature. Remarkable  $T_c$  enhancement is seen by applying a pressure of 3.0 GPa. Pressure application enhances  $1/T_1T$  just above  $T_c$ , whereas it suppresses  $1/T_1T$  at high temperatures. The behavior at temperatures above  $T_c$  originates not from the AF fluctuation but from peculiarities of the band structure as described in the following section.

#### IV. BAND STRUCTURE

The qualitatively different  $T$ - and  $P$ -dependence of  $1/T_1T$  can be explained by the band calculations [19, 20]. According to the band calculations, the AF fluctuation originates from the nesting between hole and electron pockets in the lightly doped regime, as illustrated in Fig. 1(d). In the underdoped regime ( $x = 0.08$ ), the weak Curie-Weiss behavior arises from weak nesting originating from an imbalance between hole and electron pockets. (see Fig. 1(e).) With increasing doping level,  $\gamma$  Fermi surface, a hole pocket near the  $\Gamma'(\pi, \pi)$  point in the unfolded Brillouin zone, vanishes around  $x = 0.10$  [14]. However, states near the  $\Gamma'(\pi, \pi)$  point just below the Fermi level contribute to the density of states  $D(\varepsilon_F)$  at high temperature. The  $T$ -dependent  $D(\varepsilon_F)$  gives rise to the monotonous increase in  $1/T_1T$  ( $\sim D(\varepsilon_F)^2$ ). The band-structure effect disappears at low temperatures, and other hole pockets,  $\alpha_1$  and  $\alpha_2$  surfaces around the  $\Gamma(0, 0)$  point, are expected to become small [21]. Therefore, a plateau in  $1/T_1T$  just above  $T_c$  originates from  $D(\varepsilon_F)$  at the electron pocket,  $\beta$  surface around the M point. The remarkable  $T_c$  enhancement due to pressure application is attributable to an increase in  $D(\varepsilon_F)$  at the  $\beta$  surface. Based on the band calculations, the  $1/T_1T$  components coming from  $T$ -dependent and  $T$ -independent  $D(\varepsilon_F)$  have different origins. This could explain why  $1/T_1T$  exhibits a qualitatively different pressure response

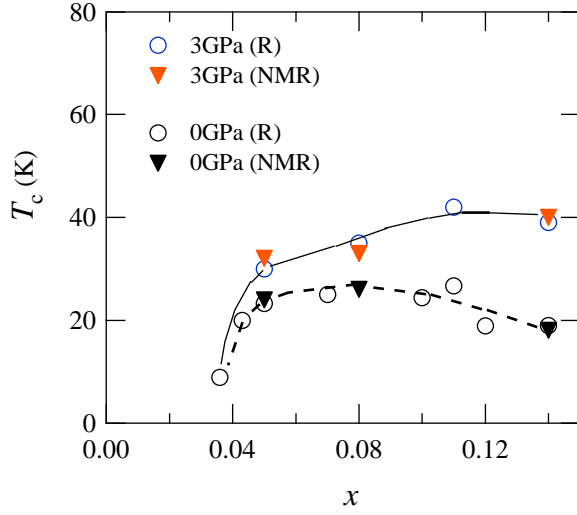


FIG. 2:  $T_c$  determined by the resistivity and  $1/T_1T$  at ambient pressure and 3 GPa. The values of  $T_c$  shown by arrows in Figs. 1(a)-(c) are plotted by triangles.

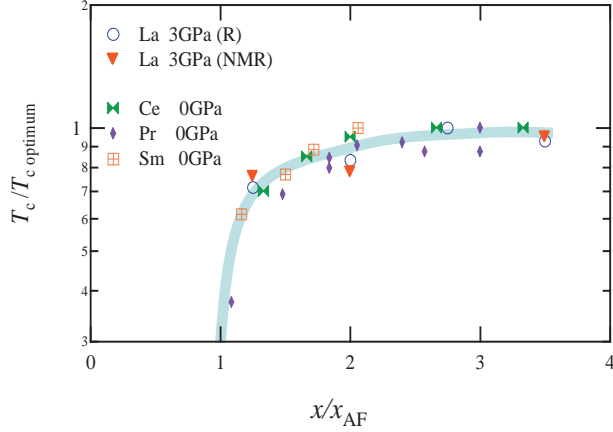


FIG. 3:  $T_c$  for various  $R\text{FeAsO}_{1-x}\text{F}_x$ .  $T_c$  and  $x$  are normalized by the optimal  $T_c$  and the antiferromagnetic phase boundary  $x_{AF}$ , respectively. Blue circles and red triangles represent  $T_c$  determined from the resistivity and  $1/T_1T$  at 3 GPa, respectively.

between low and high temperatures, as shown in Fig. 1(c):  $1/T_1T$  at high temperature is suppressed by applying pressure, whereas the plateau in  $1/T_1T$  is enhanced by applying pressure.

## V. DISCUSSION

The values of  $T_c$  determined from the onset of the resistivity and  $1/T_1T$  (arrows in Figs. 1(a)-(c)) are plotted in Fig. 2. Pressure application enhances low-frequency AF fluctuation in the underdoped regime. However, the increase in  $T_c$  is small. As the figure shows, superconductivity with  $T_c \geq 40K$  develops in the overdoped regime away from the strong AF fluctuation caused by pressure application. This fact calls into question the strong interplay between AF fluctuation and superconductivity. Thus, the question of whether the features observed in the overdoped regime are common to the other 1111 series arises.

The  $T - x$  phase diagram at 3.0 GPa is reminiscent of diagrams of the Ce, Pr and Sm 1111 series at ambient pressure in that  $T_c$  hardly drops to below 40 K even in the heavily doped regime, and the highest  $T_c$  is realized away from the AF phase. Fig. 3 shows a phase diagram normalized by the doping levels,  $x_{AF}$ , at which the AF phase vanishes. The values of  $x_{AF}$  are estimated as 0.04, 0.06, 0.075, and 0.04 for the La, Ce, Pr, and Sm 1111 series, respectively [1-7]. The phase diagram includes some ambiguity in the determination of  $x_{AF}$ . However, Fig. 3 allows comparison of the SC phase boundary because differences due to  $x$ -estimation methods are excluded to some extent. As the figure shows, the  $x/x_{AF}$  dependence of  $T_c$  normalized by the optimal  $T_c$  is almost the same for the 1111 series with high  $T_c$  above 40 K.

The similarity between the La1111 series at 3.0 GPa and the other 1111 series is well understood if the pnictogen height from the basal plane of iron determines  $T_c$ , as suggested by a theoretical investigation [14]. According to x-ray diffraction measurements under pressure by Garbarino, *et. al.*, pnictogen height increases with increasing pressure, and the lattice constant shrinks as well [22]. The same changes occur by complete replacement of rare-earth ions: the pnictogen height increases in the order of La, Ce, Nd, and Sm, and the lattice constants also shrink in the same order [3, 6, 23-25]. The La1111 series at 3.0 GPa ( $T_c = 40$  K) corresponds to the Ce1111 series at ambient pressure. The pnictogen height and lattice parameter of the Ce1111 series are 0.1565 and 3.97 Å, respectively [6]. According to the x-ray diffraction measurements on the La 1111 series, the former and latter are estimated to be 0.158 and 3.97 Å, respectively, at 3.16 GPa [22]. The agreement is fairly good, therefore, the La1111 series at 3.0 GPa and the Ce1111 series at ambient pressure are equivalent, and the phase diagram determined under pressure is common to the 1111 series with high

$T_c$  above 40 K. In some respects, pressure application to the La1111 series is very useful to investigate the high- $T_c$  mechanism in the other 1111 series with  $T_c \geq 40$  K, because in the other 1111 series magnetic fluctuation arising from rare-earth ions predominates, which prevents the extraction of AF fluctuation arising from the basal planes of iron.

## VI. SUMMARY

In summary, the relationship between the AF fluctuation and superconductivity was investigated by using NMR under high pressure, suggesting that high  $T_c$  above 40 K in the 1111 series originates not from the AF fluctuation but from  $D(\varepsilon_F)$  at the electron pocket around the M point.

- 
1. Y. Kamihara *et. al.*, J. Am. Chem. Soc. **130**, 3296 (2008)
  2. H. Luetkens *et. al.*, Nature Materials, **8**, 305 (2009)
  3. Q. Huang *et. al.*, Phys. Rev. B **78**, 054529 (2008)
  4. Y. Kamihara *et. al.*, N. J. Phys. **12**, 033005 (2010)
  5. C. Hess *et. al.*, Europhys. Lett. **87**, 17005 (2009)
  6. J. Zhao *et. al.*, Nature Materials, **7**, 953 (2008)
  7. C. R. Rotundu *et. al.*, Phys. Rev. B **80**, 144517 (2009)
  8. H. Chen *et. al.*, Europhys. Lett. **85**, 17006 (2009)
  9. B. Lv. M. Gooch *et. al.*, New. J. Phys. **11**, 025013 (2009)
  10. F. Rullier-Albenque *et. al.*, Phys. Rev. Lett. **103**, 057001 (2009)
  11. H. Takahashi *et. al.*, Nature **453**, 376 (2008)
  12. H. Okada *et. al.*, J. Phys. Soc. Jpn. **77**, 113712 (2008)
  13. C. H. Lee *et. al.*, J. Phys. Soc. Jpn. **77**, 083704 (2008)
  14. K. Kuroki *et. al.*, Phys. Rev. B **79**, 224511 (2009)
  15. S. Onari, and H. Kontani, Phys. Rev. Lett. **103**, 177001 (2009)
  16. H. Kontani, and S. Onari, Phys. Rev. Lett. **104**, 157001 (2010)
  17. T. Nakano *et. al.*, Phys. Rev. B **81**, 100510(R) (2010)
  18. K. Tatsumi *et. al.*, J. Phys. Soc. Jpn. **78**, 023709 (2009)

19. K. Kuroki *et. al.*, Phys. Rev. Lett. **101**, 087004 (2008)
20. I. I. Mazin *et. al.*, Phys. Rev. Lett. **101**, 057003 (2008)
21. H. Ikeda *et. al.*, Phys. Rev. B **81**, 054502 (2010)
22. G. Garbarino *et. al.*, Phys. Rev. B **78**, 100507(R) (2008)
23. J. Zhao *et. al.*, Phys. Rev. B **78**, 132504 (2008)
24. Y. Qiu *et. al.*, Phys. Rev. Lett. **101**, 257002 (2008)
25. S. Margadonna *et. al.*, Phys. Rev. B **79**, 014503 (2009)